Time-Dependent Resilience Assessment of Seismic Damage and Restoration of Interdependent Lifeline Systems

Szu-Yun Lin, S.M.ASCE[1]; and Sherif El-Tawil, Ph.D., P.E., F.ASCE[2]

Abstract: A simulation of the resilience of lifeline systems in a test bed subjected to a series of seismic events is presented in this paper. The simulation framework is comprised of a group of independent simulators that interact through a publish–subscribe pattern for data management. The framework addresses the spatial and time-dependent interactions that arise between lifeline systems as a hazard and subsequent restoration processes unfold. The simulation results quantify how operability loss and recovery time may be underestimated if the interdependencies between lifeline systems are not properly taken into account. The effect of insufficient resources on recovery was investigated, and it was demonstrated that among the six resource allocation strategies studied, the time-varying strategies that are responsive to actual conditions on the ground had a better effect on resilience. This paper demonstrates the power of connecting simulators using the publish–subscribe method in order to account for multiscale interdependency and time-dependent effects on community resilience.
DOI: 10.1061/(ASCE)IS.1943-555X.0000522.

Motivation and Objectives for the Study

Modeling a disaster and subsequent recovery efforts is complicated by the differing time scales for the various phases of the process, that is, seconds or minutes as a hazard unfolds versus days or months as emergency efforts and recovery take place. As a result, studies that model the multiple phases of a disaster within one overarching simulation are rare due to the challenge of integrating different simulation models with disparate temporal and spatial scales.

A common assumption in resilience studies is that a hazard occurs during one analysis step, that is, virtually instantaneously. In reality, hazards unfold in a finite amount of time. Accounting for how a hazard unfolds and affects infrastructure systems that interact with one other can yield new insights into how interdependencies affect community resilience. This is especially important for situations such as long-period disasters that overlap with short-term recovery efforts [e.g., the emergency response to a hurricane (Schmeltz et al. 2013)], short-period disasters that interact with an ongoing recovery efforts (e.g., an aftershock affecting the recovery effort associated with a main shock), or multiple disasters occurring in a specific locale [e.g., an earthquake followed by a tsunami (Moreno and Shaw 2019)].

Given the paucity of studies in this area, the objective of this research was to conduct an analysis that explicitly addressed the spatial and temporal progression of earthquake-induced damage and the postdisaster restoration effort. After a review of the literature, the methodology and framework are introduced and a case study of three interdependent lifeline systems subjected to two successive earthquakes is presented. Last, the applicability and limitations of the framework are discussed.

Background

There is broad consensus that the interdependencies that exist between the lifeline systems of a society can significantly impact the resilience of communities facing natural and man-made hazards (Cutter et al. 2003; NER 2011; Cimellaro et al. 2016).

Various methods for classifying interdependencies have been proposed (Zimmerman 2001; Rinaldi et al. 2001; Dudenhoeffer et al. 2006; Zhang and Peeta 2011), and different computational modeling approaches have been used to study the effects of interdependencies on community resilience. Eusgeld et al. (2008) and Ouyang (2014) categorized these approaches into several types: empirical, agent-based, system dynamics, economic theory, network-based approaches, and other techniques. The two most often-used approaches for modeling community resilience are agent-based models and network-based methods. Agent-based models are powerful because they can capture pertinent behavior at the component level (Barton et al. 2000; Schoenwald et al. 2004; Reilly et al. 2017). Their versatility is, however, marred by their computational expense. Network-based approaches are computationally expedient. They are widely used in lifeline system modeling because these types of systems can typically be represented as a network graph with nodes and links (Hernandez-Fajardo and Dueñas-Osorio 2013; Guidotti et al. 2016). A more detailed discussion of the various modeling techniques can be found in Eusgeld et al. (2008), Ouyang (2014), and Lin et al. (2019).

Numerous studies have been conducted to evaluate the resilience of communities subjected to hazards. The PEOPLES resilience framework (Renschler et al. 2010; Cimellaro et al. 2016) includes seven dimensions for assessing community resilience: population and demographics, environmental and ecosystem, organized governmental services, physical infrastructures, lifestyle and community competence, economic development, and social-cultural capital. Miles and Chang (2011) introduced a simulation

[1]Ph.D. Student, Dept. of Civil and Environmental Engineering, Univ. of Michigan, Ann Arbor, MI 48109-2125 (corresponding author). ORCID: https://orcid.org/0000-0001-5369-2571. Email: sylin@umich.edu

[2]Professor, Dept. of Civil and Environmental Engineering, Univ. of Michigan, Ann Arbor, MI 48109-2125. ORCID: https://orcid.org/0000-0001-6437-5176. Email: eltawil@umich.edu

Note. This manuscript was submitted on January 21, 2019; approved on July 15, 2019; published online on December 26, 2019. Discussion period open until May 26, 2020; separate discussions must be submitted for individual papers. This paper is part of the ***Journal of Infrastructure Systems***, © ASCE, ISSN 1076-0342.

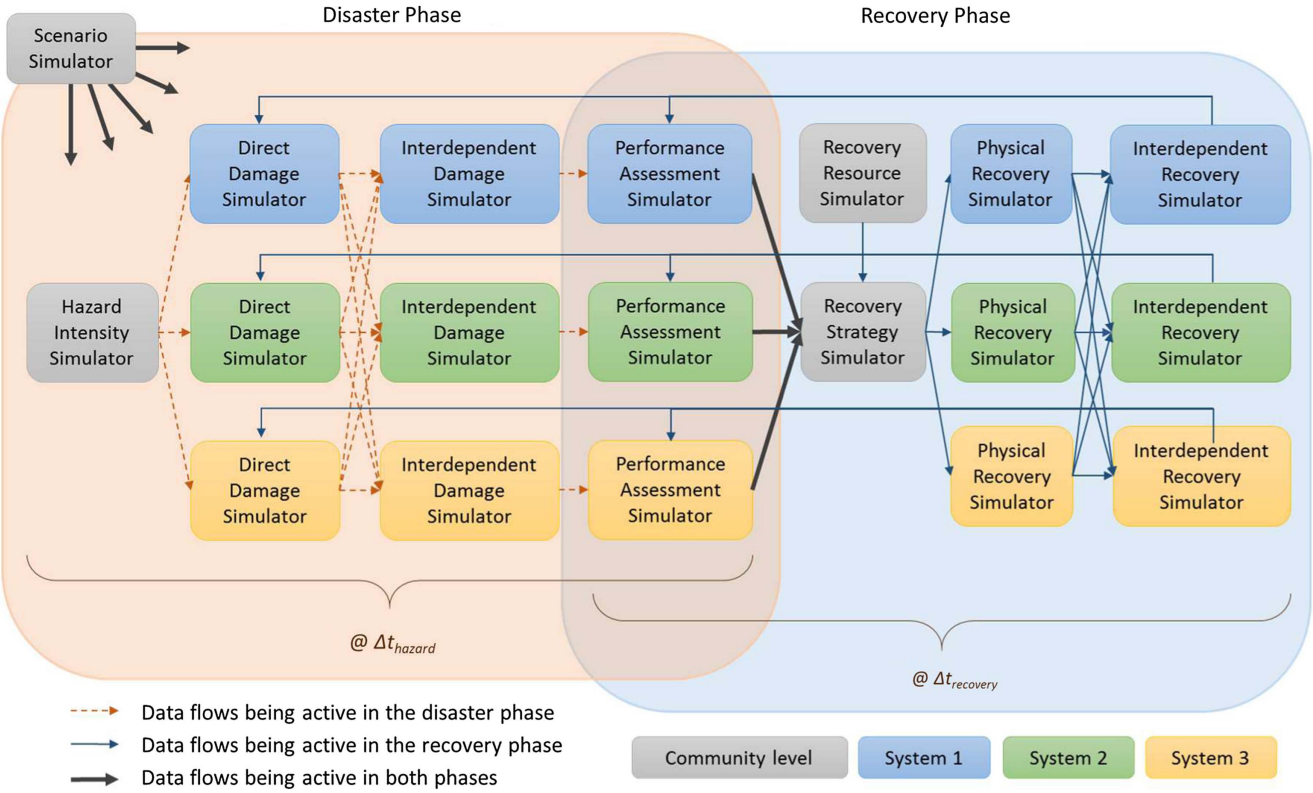

Fig. 1. Simulation framework and message flow.

model named ResilUS that was built on their previous efforts (Chang and Miles 2004; Miles and Chang 2007) and provided an implementation of the 1994 Northridge earthquake. The NIST-funded Center for Risk-Based Community Resilience Planning has developed the Interdependent Networked Community Resilience Modeling Environment (IN-CORE), which some studies have demonstrated on a virtual test bed community called Centerville (Ellingwood et al. 2016; Guidotti et al. 2016; Lin and Wang 2016; Cutler et al. 2016). The Civil Restoration with Interdependent Social Infrastructure Systems (CRISIS) model (Loggins et al. 2019) mapped services provided by civil infrastructure to the performance of social infrastructure systems and aimed to find restoration schemes that optimize the performance of social systems. As Koliou et al. (2018) concluded, there are only a handful of frameworks that can account for the multidisciplinary and multiscale nature of community resilience in time-varying resilience analyses. The methodology employed in this research is geared toward addressing these gaps in the literature.

Computational Framework

Lin et al. (2019) provides a detailed description of the modeling environment and publish–subscribe data transmission pattern used in this work. Fig. 1 shows how the various simulators employed herein interact together, and Fig. 2 illustrates the publish–subscribe relationship between the simulators. Each simulator publishes its results (in a "message") to a corresponding "channel." Other simulators, which need the information, subscribe to the channels and receive published messages from them. This method of data management is used in computer science to compose complex simulations from a set of individual, interacting simulators (Lin et al. 2019). Modifiability and scalability are the key advantages of this methodology. In particular, it allows simulators to be replaced based on different theories or algorithms and permits new simulators to be added to existing simulation frameworks, allowing for increasing levels of complexity.

The messages published during a disaster event are described in Table 1 and the corresponding publishers and subscribers are listed in Table 2. The run-time interface shown in Fig. 2 manages the flow of messages, permitting the analysis to proceed in a decentralized and scalable manner. Although Figs. 1 and 2 show the framework for the case study considered herein, which contains three interdependent systems, it can be extended in a straightforward manner to handle other situations with more interacting systems and simulators.

The scenario simulator in Fig. 1 describes the basic configuration information, specifically the location and characteristics of

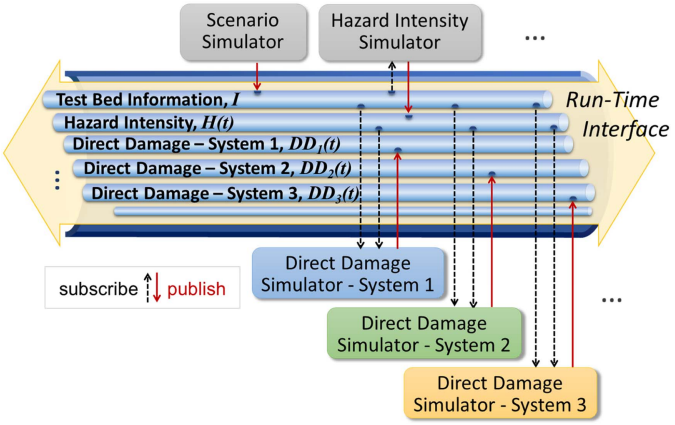

Fig. 2. Publish–subscribe concept for data exchange.

J. Infrastruct. Syst., 2020, 26(1): 04019040

Table 1. Message types published during a disaster event

Code	Message description
I	Configuration of and information on test bed that does not change with time
$H(t)$	Hazard intensity measures at all locations of interest at time t
$DD_i\ (t)$	Damage status of components directly induced by a hazard at time t
$ID_i(t)$	Damage status of components considering interdependency effects at time t
$P_i\ (t)$	System performance measures at time t
$RS(t)$	Total available recovery resources and constraints at time t
$S(t)$	Allocation strategy of recovery resources at time t
$R_i(t)$	Physical recovery status of components at time t
$IR_i\ (t)$	Recovery status of components considering interdependency effects at time t

Note: Subscript i indicates messages produced by system i.

Table 2. Messages published or subscribed to by the simulators

Simulator	Message published	Messages subscribed to
Scenario simulator	I	—
Hazard intensity simulator	$H(t)$	I
Direct damage simulator i	$DD_i\ (t)$	I, $H(t)$, $IR_j\ (t)$, $j = 1, 2, \ldots$
Interdependent damage simulator i	$ID_i(t)$	I, $DD_j\ (t)$, $j = 1, 2, \ldots$
Performance assessment simulator i	$P_i\ (t)$	I, $ID_j(t)$, $IR_j\ (t)$, $j = 1, 2, \ldots$
Recovery resource simulator	$RS(t)$	I
Recovery strategy simulator	$S(t)$	I, $P_j\ (t)$, $j = 1, 2, \ldots$
Physical recovery simulator i	$R_i(t)$	I, $S(t)$
Interdependent recovery simulator i	$IR_i\ (t)$	I, $R_j(t)$, $j = 1, 2, \ldots$

Note: Subscript i refers to system i.

utility facilities and the connectivity between them. Such information is published at the beginning of simulations and assumed not to change with time. Once a disaster occurs (in the disaster phase), the hazard intensity simulator provides information about the hazard, such as the magnitude and epicenter of an earthquake in a seismic disaster. Although this paper only focuses on seismic events, the hazard intensity simulator could also provide information about storm track and intensity if a hurricane hazard were of concern. The simulator provides specific hazard information at all locations of interest to other simulators—for example, ground motions at a given location.

The direct damage simulator calculates the physical damage of components directly induced by a hazard regardless of the influence of other infrastructure systems. Damage can be evaluated using empirical models, fragility curves, or detailed finite-element models. The fact that the simulation framework does not care about the specific method by which damage is assessed is a key strength of the methodology. The interdependent damage simulator addresses the effects of interdependencies on damage occurrence. Interdependencies come in many varieties. They can be functional, spatial, or both (Zimmerman 2001); cyber, geographic, and logical (Rinaldi et al. 2001); physical, geospatial, policy, and informational (Dudenhoeffer et al. 2006); functional, physical, budgetary, market, and economic (Zhang and Peeta 2011). The performance assessment simulator assesses system performance and is a key determinant for formulating a recovery strategy.

In the recovery phase, the recovery resource simulator estimates the amount of resources, such as labor, equipment, materials, and budget, that can be used for lifeline restoration. The recovery strategy simulator allocates limited recovery resources to the systems based on a given recovery strategy, which may depend on the damage status and performance of the systems. The influencing factors and strategy for the allocation of recovery resources may change during the recovery process. Such time-dependent effects are a key focus of this research; the study of such effects is enabled by the distributed simulation methodology adopted in this work. Once damage occurs, the physical recovery simulator determines the reconstruction priority of damaged components based on their damage situation and degree of importance in the system, and estimates the required time for restoration. During every recovery period, the simulator further distributes recovery resources allocated from the recovery strategy simulator to each damaged component in order of priority, that is, system level to component level. Then, within every recovery step, the physical recovery simulator decides whether reconstruction progress advances forward or pauses according to whether a component has enough allocated resources.

The interdependencies between the various systems must be considered not only as a hazard unfolds but also during the recovery process. For example, one component in a network system may have completely recovered from damage inflicted by a hazard but still cannot function properly due to its dependency on another still-damaged system. Therefore, like the interdependent damage simulator, the interdependent recovery simulator considers interdependent behaviors across systems and updates the recovery status and functionality of components.

The simulators used in this work span different spatial scales: whole community, infrastructure system, and structural component. Community-level simulators affect large geographic areas (e.g., the scenario simulator and hazard intensity simulator) or represent decisions that address a large part of a community (e.g., the recovery strategy simulator). System-level simulators address physical infrastructure systems such as lifeline networks. The lowest spatial level pertains to components of the various infrastructure systems, such as residential buildings or pumping stations. The times scales considered herein also vary widely. As illustrated in Fig. 1, the time scale as the disaster phase unfolds Δt_{hazard} is several orders of magnitude smaller than the time step during the recovery phase $\Delta t_{\text{recovery}}$. The framework employed in this work allows for the possibility of subsequent hazards to occur—for example, an aftershock that occurs during an ongoing recovery progress.

Shifts between the disaster and recovery phases are controlled by the performance assessment simulator, which is involved in both phases. This simulator judges the beginning and end of a disaster by interpreting the received damage messages and provides the latest system performance to the recovery strategy simulator. As shown in Fig. 1, in the disaster phase, the performance assessment simulator calculates system performance based on damage status provided by the interdependent damage simulator, and in the recovery phase, it continues to update system performance according to the recovery status from the interdependent recovery simulator. The direct damage simulator also subscribes to the recovery status provided by the interdependent recovery simulator, although it does not publish anything during the recovery phase. This is because it needs to know the latest recovery status in order to assess the capacity reduction in components that are not yet fully repaired when the next disaster occurs.

The computational framework handles several types of interdependencies. Most importantly, the interdependencies between system performances and community-level recovery strategy are accounted for in a dynamic sense. In other words, recovery strategy can evolve depending on system performance at a given time.

Second, because additional disruptions can occur during an ongoing recovery process, the ability of each component to resist new demands caused by subsequent hazards may be affected by damage from a previous event and unfinished rehabilitation efforts. Last, interdependencies can occur between components of different lifeline systems and must be accounted for. These interdependent relationships are shown in Fig. 1 by the interlaced lines joining the direct damage simulator and the interdependent recovery simulator or joining the physical recovery simulator and the interdependent recovery simulator.

The extensibility and flexibility of the computational framework for modeling various types of interdependencies between disparate systems are the key strengths of the platform. For example, if new interacting systems are added, the interdependent damage/recovery simulators merely need to subscribe to the new direct damage simulators or physical recovery simulators on which they depend. No changes need to be made to other simulators in the system. The publish–subscribe approach used in this work eliminates the need for using interdependency matrices, which are commonly used to specify the relationships between different pairs of networks. The limitations associated with using interdependency matrices are discussed in Lin et al. (2019).

Case Study: Seismic Damage and Recovery of Lifeline Systems in Shelby County, Tennessee

Shelby County, Tennessee, which is close to the southwest end of the New Madrid seismic zone (NMSZ) has been used as a test bed in many studies. Dueñas-Osorio et al. (2007), Adachi and Ellingwood (2008), and Hernandez-Fajardo and Dueñas-Osorio (2013) studied the interdependent response of water and power systems in Shelby County under earthquake demands. Adachi and Ellingwood (2009) assessed the performance of its water system under spatially correlated seismic intensities. Song and Ok (2010) analyzed multiscale effects on system reliability of the gas transmission network in Shelby County. González et al. (2016) developed restoration strategies that took into account the interdependencies between the water, power, and gas network systems in Shelby County.

In a departure from previous studies, the computational framework was applied to Shelby County, Tennessee in order to demonstrate how it can be used to investigate earthquake-induced damage and the subsequent recovery progress, which itself is interrupted by an aftershock (first shock—short term recovery effort—second shock—long term recovery effort). The framework was applied to three interdependent lifeline systems in order to demonstrate its scalability. Unlike the aforementioned studies, which merely focused on one of the phases in a hazard event, that is, the disaster process or the recovery period, this study presents an overall simulation that addresses the disaster and postdisaster phases in an integrated manner. Another key advantage of the framework is that it naturally combines simulators that have disparate temporal and spatial scales.

To capture the uncertainty in the seismic damage and the restoration process, Monte Carlo simulations were performed, and the means of the results are presented. Studies with 300, 500, and 1,000 simulations were conducted to select a reasonable number of simulations. The studies showed that the average relative differences of the first to the last were 4.75% (300 runs versus 1,000 runs) and 0.21% (500 runs versus 1,000 runs). Therefore, the number of Monte Carlo runs was set to 500.

The following section describes the details of the simulators shown in Fig. 1 and discussed previously.

Scenario Simulator

The scenario simulator provides configuration information about the lifeline systems considered herein. The systems of interest include the electric power system (EPS), water distribution system (WDS), and natural gas system (NGS), which are operated by the Memphis Light, Gas, and Water (MLGW) division. The topological configuration of the networks was adapted from Chang et al. (1996), Dueñas-Osorio et al. (2007), and Song and Ok (2010). Fig. 3 shows the topologies and critical components of the power, water, and gas network systems in Shelby County. The gate stations in EPS and NGS and the elevated tanks and pumping stations in WDS are supply nodes. The 23 kV/12 kV substations in EPS, the intersection nodes in WDS, and the regulator stations in NGS are demand nodes. The intersection nodes in EPS and NGS and all directed arcs represent the transmission components.

Hazard Intensity Simulator

The scenario earthquakes were assumed to have an epicenter at 35°18'N and 90°18'W; the same assumption was made in Adachi and Ellingwood (2009). Ground motions designated RSN-5223 (designated EQ1) and RSN-6536 (designated EQ2) from PEER (2018) were used in this study to represent feasible seismic activity. The ground motion records, which have a 0.01-s time interval, were scaled to peak ground acceleration (PGA) at the center of Memphis (35°08'N and 89°59'W; i.e., 33 km from the epicenter). The PGA values were 0.202 and 0.341 g for EQ1 and EQ2, respectively. These values were chosen based on USGS (2018) for earthquakes with a 10% probability of exceedance in 50 years (10/50) and a 5% probability of exceedance in 50 years (5/50).

Ground motion attenuation was assumed to follow the model proposed by Atkinson and Boore (1995). Although the attenuation relationships were proposed only for the PGA, the model was assumed to be applicable to the entire acceleration record as plotted in Fig. 4 and to depend only on the distance to the epicenter. Although the assumptions related to the hazard were made for convenience, the hazard intensity simulator can be adjusted in the future once more data or new models become available.

Direct Damage Simulator

Direct damage occurs if the hazard intensity, as computed by the hazard intensity simulator, exceeds the capacity of a component. Four damage states are considered: minor, moderate, extensive, and complete. These states are irreversible and occur in sequential order. The capacity of each component is determined at the beginning of each realization in the Monte Carlo simulation. Lognormal fragility functions were used to estimate the capacities associated with different damage states for different types of utility facilities. The fragility functions were adopted from the Hazards US Multi-Hazard (HAZUS-MH) technical manual (FEMA 2003), and their parameters are listed in Table 3. It was assumed that damage to EPS can be assessed from the gate stations and substations, which are the most critical equipment for the functionality of a power system (Shinozuka et al. 2005). The intersection nodes in all networks added for dividing the transmission lines and pipelines were assumed to be not vulnerable to earthquakes (Fig. 3).

As discussed in FEMA (2003), the rate of occurrence of pipeline failures per unit length is known as the repair rate and is computed via Eq. (1), in which the unit for peak ground velocity (PGV) is cm/s. The probability that the number of pipe breaks N_B equals b within a pipeline segment of length L can be expressed as shown in Eq. (2), and the probability of pipeline breakage is shown in Eq. (3)

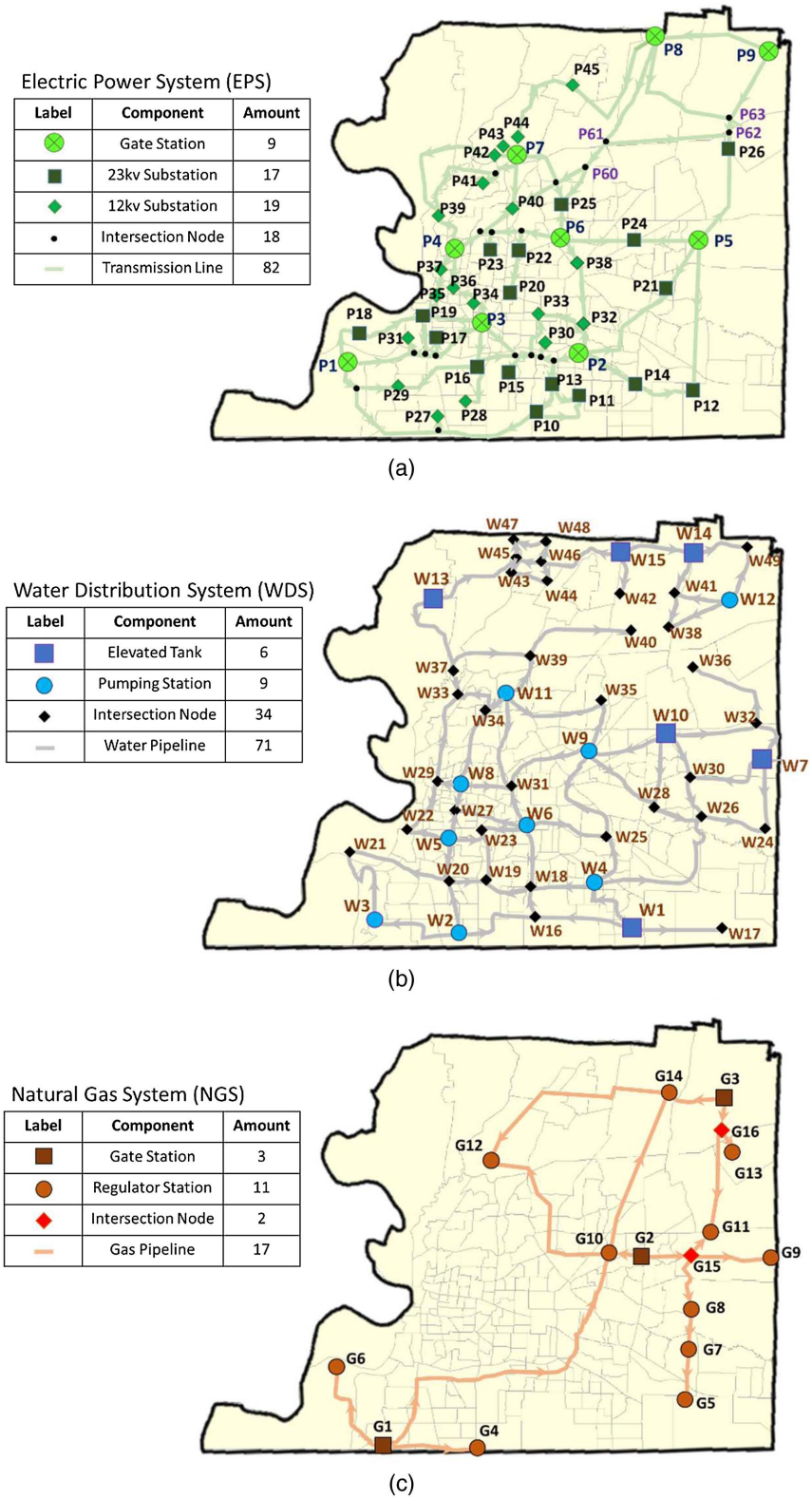

Fig. 3. Topological configuration of the lifeline systems in Shelby County, Tennessee: (a) electric power; (b) water distribution; and (c) natural gas system. [Adapted (a–c) from Chang et al. 1996; data for (a–b) from Dueñas-Osorio et al. 2007; data for (c) from Song and Ok 2010.]

$$R_{\text{rate}}[\text{repairs/km}] \cong 0.0001 \times \text{PGV}^{2.25} \quad (1)$$

$$P(N_B = b) = \frac{(R_{\text{rate}} \times L)^b}{b!} \text{e}^{-R_{\text{rate}} \times L} \quad (2)$$

$$P(N_B > 0) = 1 - P(N_B = 0) = 1 - \text{e}^{-R_{\text{rate}} \times L} \quad (3)$$

Each link in WDS and NGS is divided into several segments of approximately one km length in order to consider the scale effect (Song and Ok 2010). The PGV that corresponds with a 50%

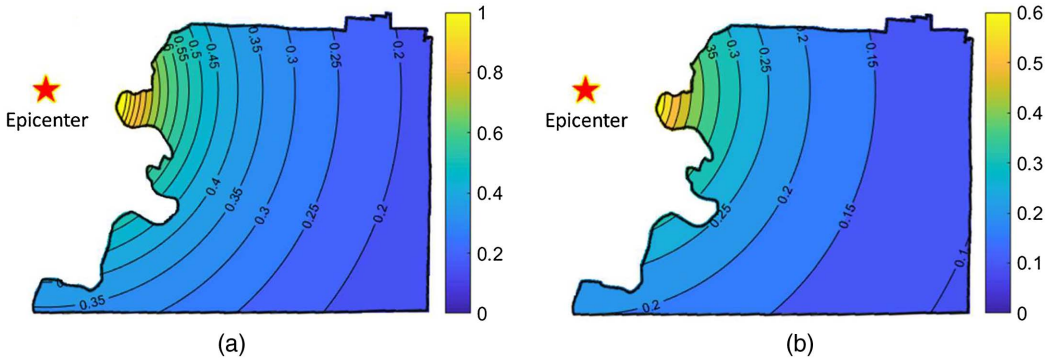

Fig. 4. Assumed attenuation of ground acceleration (unit: g) for earthquake with (a) 5%; and (b) 10% probability of exceedance in 50 years.

Table 3. Parameters of lognormal fragility functions for utility facilities

System	Components	Minor	Moderate	Extensive	Complete
EPS	Gate station	0.11 (0.50)	0.15 (0.45)	0.20 (0.35)	0.47 (0.40)
	12 kV/23 kV substation	0.15 (0.70)	0.29 (0.55)	0.45 (0.45)	0.90 (0.45)
WDS	Elevated tanks	0.18 (0.50)	0.55 (0.50)	1.15 (0.60)	1.50 (0.60)
	Pumping station	0.15 (0.75)	0.36 (0.65)	0.77 (0.65)	1.50 (0.80)
NGS	Gate station	0.15 (0.75)	0.34 (0.65)	0.77 (0.65)	1.50 (0.80)
	Regulator station	0.15 (0.75)	0.34 (0.65)	0.77 (0.65)	1.50 (0.80)

Note: All fragility functions for utility facilities are lognormal distributions with peak ground acceleration (PGA) as the engineering demand parameter. The corresponding median and lognormal standard deviation (β) are listed in the table, i.e., median (β); (unit: g).

probability of pipeline breakage was used as the capacity of each segment. Buried pipelines may also be damaged by ground failure, for example, by liquefaction. Although such situations were not considered in this case study, they could be considered in the future by adding other specialized simulators.

Component capacities are determined at the beginning of each realization based on the history of seismic activity. In the case of a first seismic event, they are considered to be damage free. When aftershocks occur during the recovery process, the integrity of the segments has already been compromised by the previous event, and component capacities are assumed to be a function of the previous damage state. In this case, the capacities of discrete components were assumed to be reduced by 40%, 20%, and 10% for extensive, moderate, and minor damage states, respectively, and the reduction ratios for broken pipelines was set to 40%, that is, an extensive damage state. These numbers can be refined in the future if the time between events is specified and the direct damage simulator and interdependent recovery simulator are able to address sequential damage effects.

Interdependent Damage Simulator

Two types of interdependencies are considered at the component-level: functional interdependencies and spatial interdependencies. A functional interdependency indicates the dependence of one system (slave nodes) on the functionality or material flow of another (master nodes). For example, pumping stations in water and gas systems rely on electric power to operate pumping machines; electric power plants rely on the water distribution system for cooling purposes and for controlling emissions of coal-based power generators. In this case study, part of the power grid depended on the natural gas system to fuel generation units. Spatial interdependency is a situation in which components from different infrastructure systems are colocated within the same geographical environment, that is, the components have spatial overlap. There is generally mutual reliance rather than master-slave relationship of functional interdependency; that is, the damage state of both nodes is the same and is governed by the node that has more severe direct damage.

Table 4. Interdependent relationships between EPS, WDS, and NGS

WDS*–EPS	EPS*–WDS	NGS*–EPS	EPS*–NGS	NGS–WDS (Mutual)
W2*–P28	P1*–W21	G6*–P18	P1*–G6	G3–W12
W3*–P29	P2*–W25	G10*–P24	P5*–G11	G14–W41
W4*–P14	P3*–W23	G12*–P44	P7*–G12	—
W5*–P17	P4*–W29	G13*–P26	—	—
W6*–P33	P5*–W30	—	—	—
W8*–P36	P6*–W35	—	—	—
W9*–P38	P7*–W39	—	—	—
W11*–P40	P8*–W42	—	—	—
W12*–P26	P9*–W49	—	—	—

Note: The left four columns indicate functional interdependencies (slave node*–master node), and the rightmost column indicates spatial interdependencies.

The conditional probability of a slave node being nonfunctional given an inoperative master node can be seen as the degree of interdependency or the coupling strength between the two nodes. Herein, the conditional failure probability of any pair of slave and master nodes is set to one, but it can be adjusted for other situations. All these interdependent relationships and the nodes involved are listed in Table 4. The interdependent damage simulator of each system only needs to know which nodes are the master nodes of its own components and subscribe to their damage conditions.

Performance Assessment Simulator

Ghosn et al. (2016) suggested that the performance measures of a network system can be divided into two categories: flow-based

and topology-based measures. Flow-based performance measures are represented by the amount of supplied flow and the proportion of satisfied customer demand. Topology-based measures are calculated based on graph theory. An abstract graph representing a lifeline network consists of supply nodes, demand nodes, and several directed links that indicate the connecting paths from supply nodes to demand nodes.

Due to a lack of information pertaining to flow capacity and demand, a topology-based metric, termed connectivity loss (CL), was selected for performance assessment in this case study. CL measures the average change in the connectivity of demand nodes to supply nodes after perturbation and is often used to assess the capability of a network system to withstand disruption (Albert et al. 2004; Dueñas-Osorio et al. 2007). At the beginning of a simulation, each lifeline system is represented as a graph with nodes and links, and the original connectivity is calculated. As the analysis progresses, inoperative components are removed from the graph, then added back when they recover. CL of a network system with N_{demand} demand nodes can be computed by Eq. (4)

$$\text{CL} = 1 - \frac{1}{N_{\text{demand}}} \sum_{i}^{N_{\text{demand}}} \left(\frac{P_i}{P_{0,i}} \right) \tag{4}$$

where $P_{0,i}$ = original number of supply nodes that connect to the ith demand node; and P_i = number of supply nodes connected to the ith demand node after a perturbation. The remaining connectivity (C) of a network is: $C = 1 - \text{CL}$.

Recovery Resource Simulator

Recovery resources are quantified as a number of resource units. A resource unit is defined as the amount of resources and budget required for an 8-person crew with accompanying repair equipment to work 12 hours (working time per day). In all of the case studies discussed subsequently, the available number of resource units R_{total} for the entire county was assumed to be a fixed value during the recovery process. In general, it is assumed that all crews have unlimited expertise, that is, they can work on all lifeline systems. However, in last case study, the crews were assumed to have different skills, and the maximum number of available crews specializing in the ith lifeline system was denoted as $R_{\text{max},i}$. Clearly, the functionality of the social infrastructure—for example, the availability of able-bodied workers who were not injured or killed in the event—affects $R_{\text{max},i}$. Although not accounted for here due to space and scope limitations, in the future, such a limitation can be accounted for through the addition of a social infrastructure simulator that, for example, accounts for worker injuries and deaths and for available funding needed to pay for repair crews.

Recovery Strategy Simulator

The recovery strategy simulator interprets the allocation strategy for recovery resources. A feasible recovery strategy is to allocate recovery resources to each system evenly regardless of their damage conditions, as stated in Eq. (5), where N_s is the number of systems and R_k is the amount of recovery resources allocated to the kth system. This strategy (the EA strategy) could represent a situation in which information about the extent of a disaster is not known. In cases in which R_{total} and N_s are fixed values during the recovery process, the EA strategy is time-independent

$$R_k(t) = \frac{R_{\text{total}}(t)}{N_s} \tag{5}$$

Another strategy (the LA strategy) is to assign resources depending on the performance of the systems in terms of connectivity loss. In this case, R_k is computed as

$$R_k(t) = \frac{CL_k(t)}{\sum_i^{N_s} CL_i(t)} \times R_{\text{total}}(t) \tag{6}$$

where CL_i = connectivity loss of the ith system. Alternatively, if the number of damaged components in each system ND_i is of concern, then a feasible strategy (the DA strategy) could be as follows:

$$R_k(t) = \frac{ND_k(t)}{\sum_i^{N_s} ND_i(t)} \times R_{\text{total}}(t) \tag{7}$$

The LA and DA strategies imply that the amount of recovery resources allocated to each system is not constant and changes over time t during the progress of recovery, reflecting the time-varying characteristic of the recovery process.

The recovery strategies applied in the example assume that systems that are more severely damaged and have worse system performance will receive more recovery resources. However, decision making during an actual disaster may be much more involved and may need to account for other factors, such as economics, politics, and societal values. In such cases, users could refine the algorithm in the recovery strategy simulator without influencing other simulators.

Physical Recovery Simulator

After a system is allocated recovery resources, the physical recovery simulator further distributes them to the damaged components. Once new damage to a system is computed, a normal distributed random variable is generated to estimate the required restoration time for each damaged component based on the restoration functions in the HAZUS-MH technical manual (FEMA 2003). Uncertainty in the recovery process is considered. The parameters of the restoration function used in the case study are summarized in Table 5. The time step of the recovery process is taken as one day, and the required resources for all types of components are assumed to be one unit per day. If a damaged component has been allocated enough resources in the recovery step (day), then its

Table 5. Parameters of restoration functions for different components

System	Components	Minor	Moderate	Extensive	Complete
EPS	Gate station	1.0 (0.5)	3.0 (1.5)	7.0 (3.5)	30.0 (15.0)
	12 kV/23 kV substation	1.0 (0.5)	3.0 (1.5)	7.0 (3.5)	30.0 (15.0)
WDS	Elevated tanks	1.2 (0.4)	3.1 (2.7)	93.0 (85.0)	155.0 (120.0)
	Pumping station	0.9 (0.3)	3.1 (2.7)	13.5 (10.0)	35.0 (18.0)
NGS	Gate station	0.9 (0.3)	3.1 (2.7)	13.5 (10.0)	35.0 (18.0)
	Regulator station	0.9 (0.3)	3.1 (2.7)	13.5 (10.0)	35.0 (18.0)

Note: All restoration functions are normal distributions. The corresponding mean and standard deviation are listed in the table, i.e., median (standard deviation); (unit: day).

repair progress will advance forward one day. Otherwise, it remains unrepaired.

The physical recovery simulator distributes allocated recovery resources to damaged components using two different strategies: randomly (the R strategy) or in order of their priority (the P strategy). In the latter case, the recovery priority of the components in each network is as follows: supply nodes, demand nodes, and links/pipelines. To simplify the simulation, resources and work crew are assumed available as soon as they are allocated, that is, the effect of transportation on work crew routing (Morshedlou et al. 2018) is not considered in this study, although it could be incorporated through the addition of other simulators.

Interdependent Recovery Simulator

The same types of interdependencies, that is, functional interdependencies and spatial interdependencies, are considered during the recovery process by the interdependent recovery simulator. The interdependent relationships (master/slave) and involved nodes are listed in Table 4. Although slave components may have completely recovered from damage inflicted by a hazard, they may not function until the master components they depend on have fully recovered. For example, the functionality of pumping stations in the water and gas systems depends both on their own repairs and on the availability of electric power. After simulation of the physical recovery, the recovery status and functionality of components is updated depending on the different interdependent behaviors across the systems.

Results and Discussion

The simulators described in the previous section were connected together using the computational framework described previously. The computational platform was then used to investigate the effects of system interdependencies, multiple shocks, recovery strategies, and allocated recovery resources on the propagation of damage during seismic events and short- and long-term recovery processes.

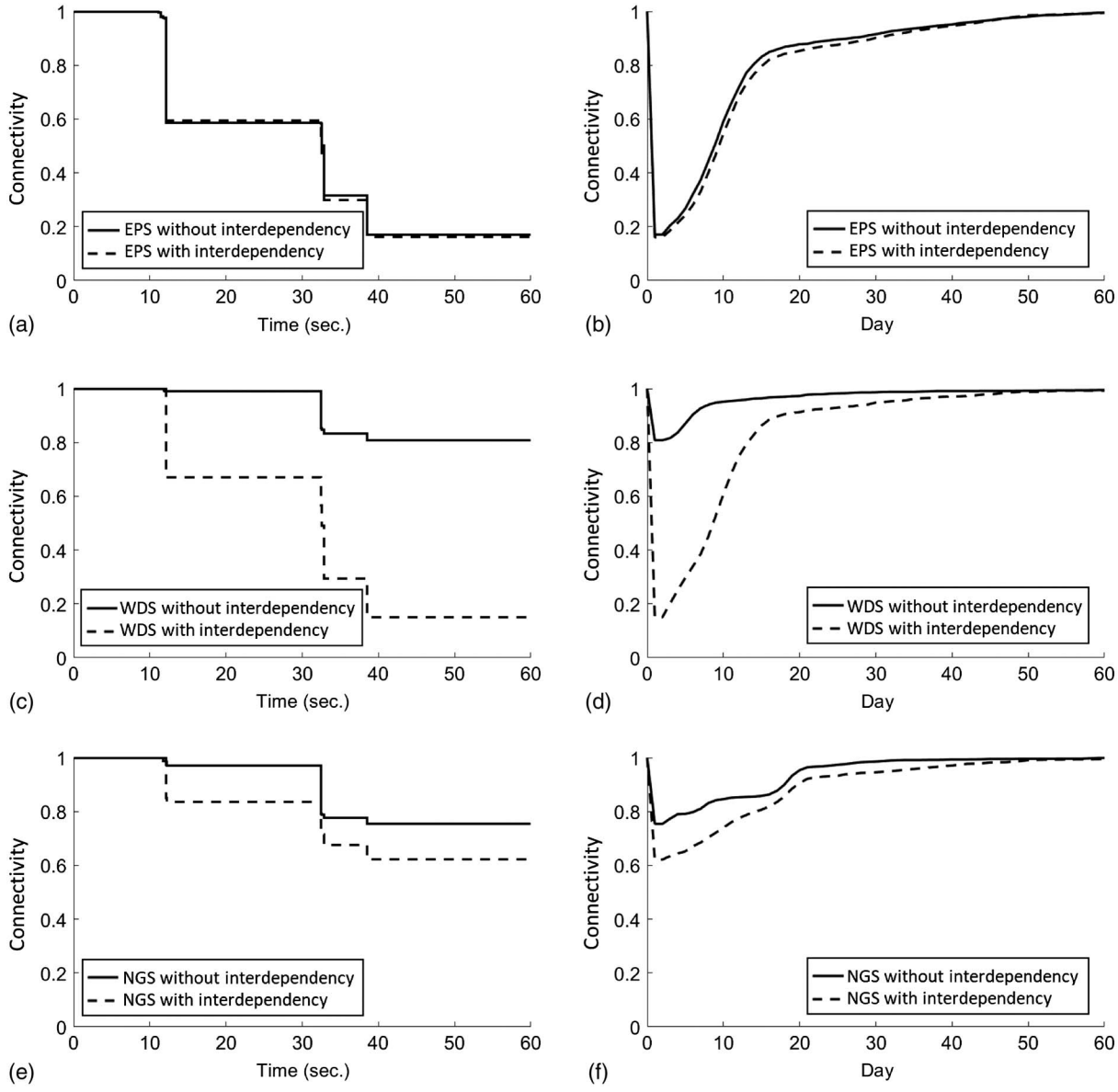

Fig. 5. Comparison of system performance with and without considering interdependencies during the earthquake and recovery processes: (a) damage curves of EPS; (b) recovery curves of EPS; (c) damage curves of WDS; (d) recovery curves of WDS; (e) damage curves of NGS; and (f) recovery curves of NGS.

Interdependencies between Lifeline Systems

First, a comparison of the performance of the three lifeline systems with and without considering the interdependencies between the systems is presented. Consider a seismic event with EQ2, $R_{\text{total}} = 45$ units/day, and crews with no limitation on their expertise. The allocation of recovery resources is based on the LA and P strategies. Fig. 5 shows the damage and recovery curves of the three lifeline systems in terms of the average system connectivity performance. The dotted lines in Fig. 5 reflect analyses that account for interdependencies, while the solid lines reflect simulations that do not account for interdependencies.

Figs. 5(a, c, and e) indicate that EPS is the system most significantly affected by the earthquake out of the three lifeline systems when interdependencies are not considered. Figs. 5(a and b) indicate that the performance of EPS is not significantly affected by interdependencies. Interdependencies are much more influential for WDS and NGS, as shown in Figs. 5(c–e). The computational results show that WDS and NGS are more dependent on EPS, and the overall recovery time, in this case, is controlled by the restoration of EPS. It is clear that the operability loss and recovery times may be significantly underestimated if the interdependencies between lifeline systems are not adequately accounted for.

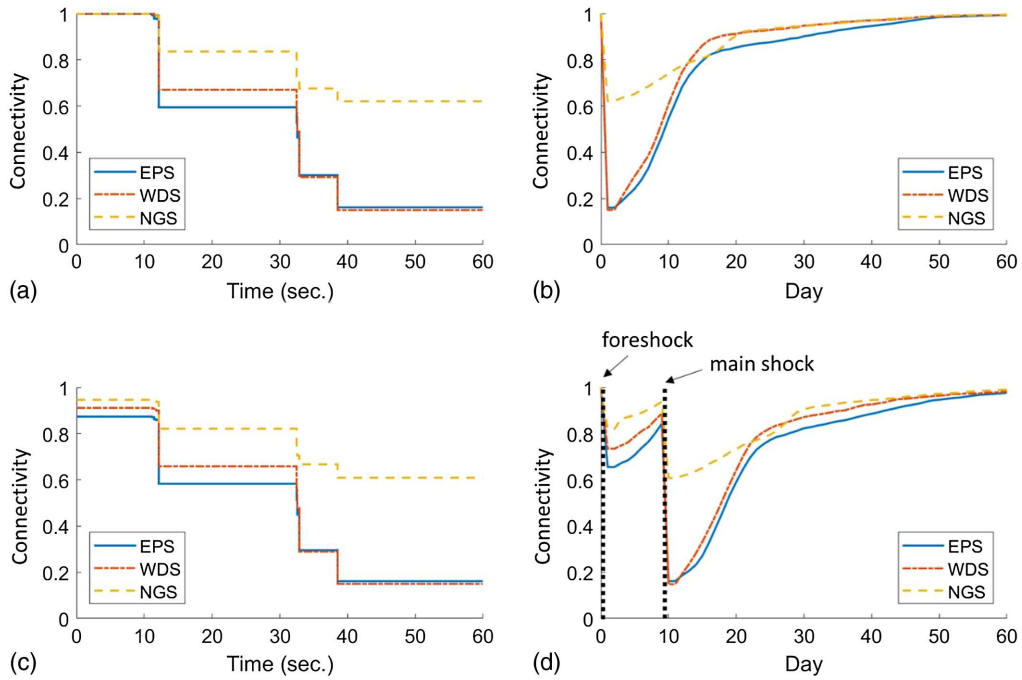

Fig. 6. Influence of foreshock on the lifeline system performance during (a) main shock without foreshock; (b) overall event without foreshock; (c) main shock affected by foreshock; and (d) overall event with foreshock.

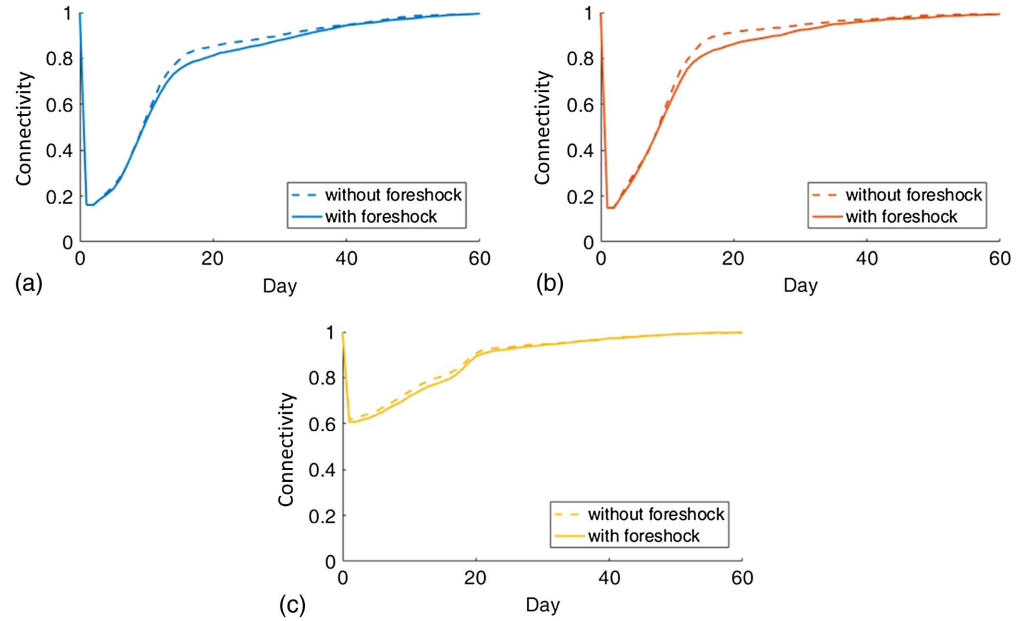

Fig. 7. Influence of foreshock on recovery after main shock: (a) EPS; (b) WDS; and (c) NGS.

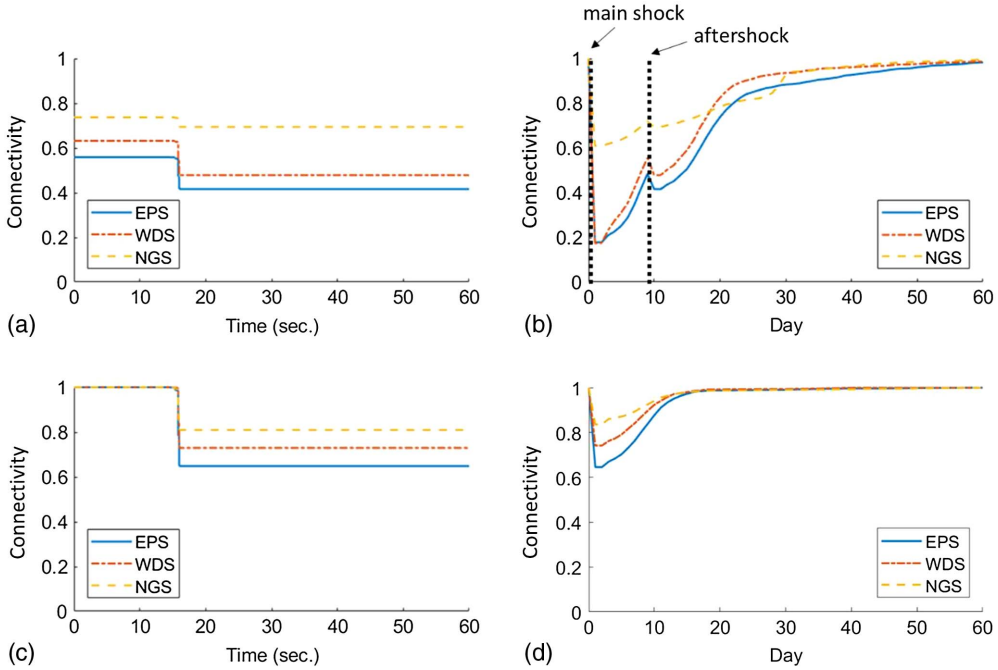

Fig. 8. Influence of aftershock on the lifeline system performance during (a) aftershock following main shock; (b) overall event (main shock followed by aftershock); (c) aftershock by itself (without considering the effect of the main shock); and (d) overall event involving only aftershock.

Influence of Foreshock

The influence of the foreshock is evaluated by considering a sequence of seismic events comprised of EQ1 followed by EQ2, $R_{\text{total}} = 45$ units/day, and crews with no limitation on their expertise. The allocation of the recovery resources is based on the LA and P strategies. The performance of the lifeline systems is indicated by the connectivity ratio, as plotted in Fig. 6. Figs. 6(a and b) pertain only to the main shock, while Figs. 6(c and d) illustrate the outcomes of EQ1 (the foreshock) leading up to EQ2 (the main shock). Figs. 6(a and c) indicate that the worst connectivity ratio of the lifeline systems is governed by the main shock, which is larger than the foreshock. However, the damage inflicted by the foreshock makes the lifeline systems more vulnerable to the later quake. As shown in Fig. 7, the recovery slows down slightly in the long-term when the foreshock is considered, because the final damage after the main shock is more severe and there are more damaged components in need of repair, which might not be fully reflected in the connectivity loss.

Influence of Aftershock

Consider a seismic event with EQ2 (main shock) followed by EQ1 (aftershock), $R_{\text{total}} = 45$ units/day, and crews with no limitation on their expertise. The allocation of recovery resources is based on the LA and P strategies. Fig. 8 shows the changes in system performance with an aftershock compared to EQ1 by itself. As shown in Figs. 8(a and b), the aftershock induces additional damage and decelerates the speed of restoration despite being smaller than the main shock. Moreover, by comparing Figs. 8(a and b) with Figs. 8(c and d), it can be seen that the damage due to the aftershock is much more serious than the damage due to a single earthquake with the same magnitude. For example, in Fig. 8(d), the remaining connectivity of EPS in the case with EQ1 by itself is about 0.64, but in the case with the aftershock, the connectivity of EPS after EQ1 (aftershock) decreases to 0.42, as shown in Fig. 8(b).

Effect of Recovery Strategies

As discussed previously, two levels of recovery strategies are proposed: community to system (EA, LA, and DA) and system to component (R and P). As a result, there are six different combinations of recovery strategies. The schemes are designated by their names—for example, EA followed by R is EA-R and LA followed by P is LA-P.

Consider a seismic sequence of events with EQ1 as a foreshock followed by EQ2 as the main shock. Resources $R_{\text{total}} = 9$ units/day, and repair crews have no limitations on their expertise. The focus is only on the connectivity performance of EPS. It is clear from Fig. 9 that the three strategies that employ the P allocation have steeper recovery curves in the early stages of reconstruction. They also have better performance in the overall resilience process. Among the six different recovery schemes,

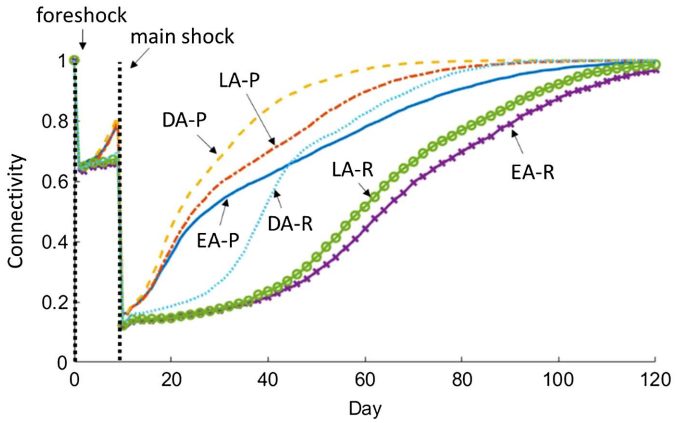

Fig. 9. Effect of different recovery strategies on the connectivity performance of EPS.

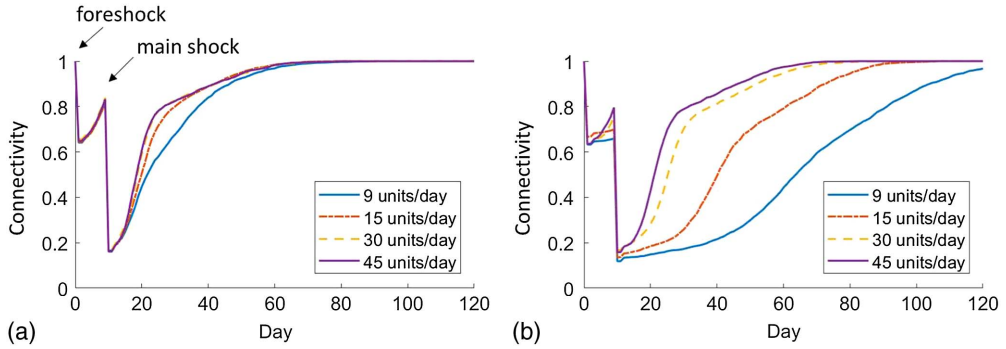

Fig. 10. Effect of recovery resources on EPS with recovery strategy: (a) DA-P; and (b) EA-R.

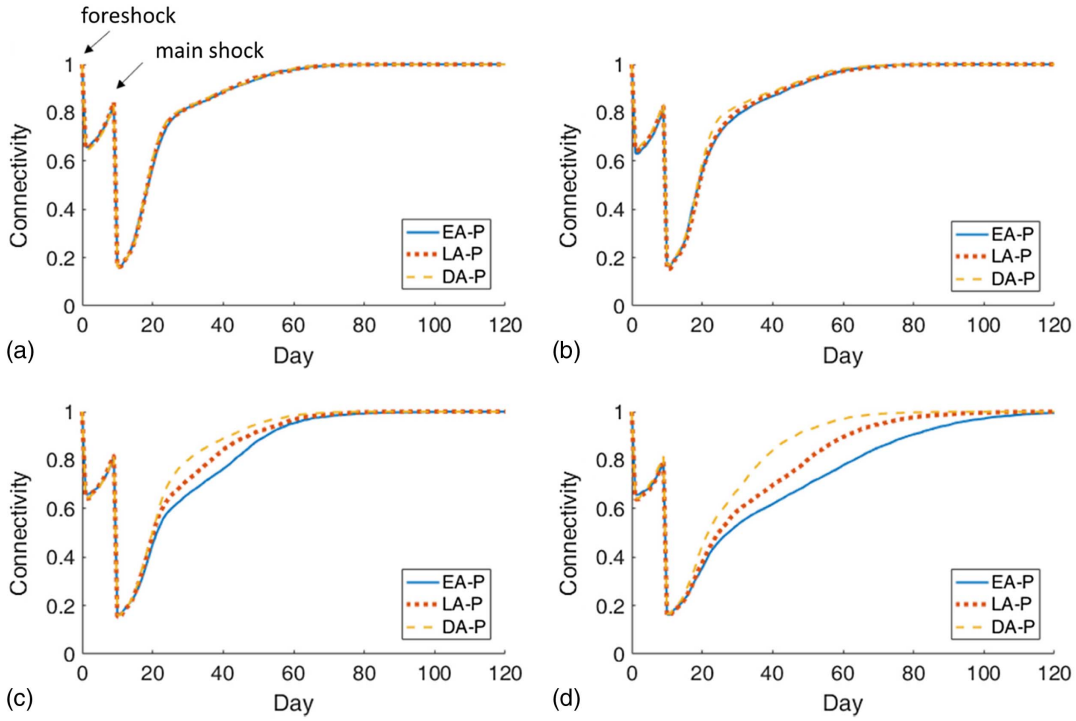

Fig. 11. The connectivity performance of EPS adopting different recovery strategies with different recovery resources with (a) 45; (b) 30; (c) 15; and (d) 9 units/day.

the EA-R scheme has the worst recovery performance. The best is DA-P.

Effect of Amount and Type of Recovery Resources

To study the effect of the amount of recovery resources, consider again a case with EQ1 as a foreshock followed by EQ2 as the main shock. In this case R_{total} varies and equals 9, 15, 30, or 45 units/day, and crews have no limitation on their expertise. Focusing again on EPS, the best (DA-P) and worst (EA-R) strategies discussed previously are employed to maximize the contrast between them, and the results are shown in Figs. 10(a and b), respectively. As expected, recovery performance improves as more recovery resources are allocated. Fig. 10 also shows that the effect of limited resources is significantly more pronounced in the lower-efficiency scheme. Fig. 11 compares the effect of the amount of resources on recovery when different strategies are employed. Again, the less efficient schemes suffer more pronounced effects when fewer resources are available.

Consider a similar study with crews that have specific (not general) expertise—for example, a crew is only able to service a particular lifeline system. Consider a seismic sequence of events with EQ1 as a foreshock, followed by EQ2 as the main shock. The DA-P strategy is applied, and two different recovery resource constraints are considered. First, funding is available to pay up to 15 repair crews per day, that is, $R_{\text{total}}(t) \leq 15$ units/day (Constraint 1). Second, the crews are specialized, with up to five crews specializing in each lifeline system, that is, $R_k(t) \leq R_{\max,k} = 5$ (Constraint 2), where $R_k(t)$ is the amount of recovery resources allocated to the kth system. Fig. 12 compares the performance of EPS with different levels of recovery resource constraints. The figure shows that the resilience of the community is overestimated if crew expertise is not account for, especially in the period between 25 and 60 days.

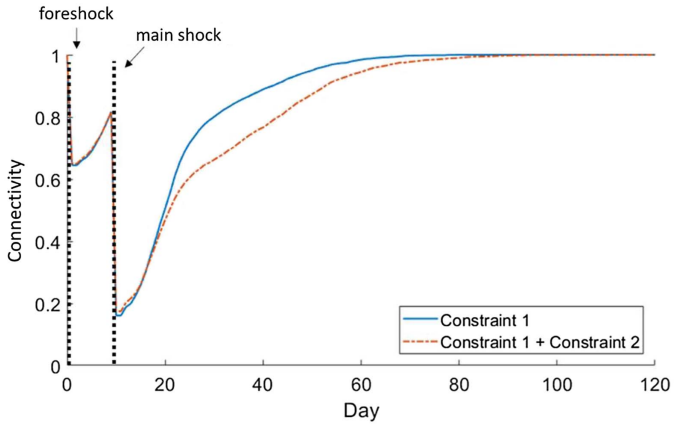

Fig. 12. Comparison of different levels of recovery resource constraints.

Summary and Conclusions

A distributed computational framework was employed to model the interactions that occur between lifeline systems during earthquakes. Various systems were modeled using simulators with disparate temporal and spatial scales. The simulators were connected through a computational platform. Shelby County, Tennessee, was used as a case study for demonstrating the ability of the framework to model the interactions between three lifeline systems. The effects of different recovery strategies on system performance were examined as the hazard unfolded and as the recovery process took place. The computational results quantified the influence of the interdependencies between the lifeline systems on the resilience of the community.

Aside from the need to account for multiscale interdependencies, the case study pointed out the necessity of time-varying analysis as the hazard unfolded and during the recovery process. The seismic hazard considered in this work occurred in just a few seconds. Nevertheless, modeling the interactions that occurred between the lifeline systems during the event provided insights into how interdependencies among infrastructure systems propagate and provided clues as to how to improve their resilience. The ability to handle differences in temporal scales between a hazard and the recovery process is one of the key advantages of the analysis, as evinced by its ability to handle aftershocks that interact with an ongoing recovery effort.

The case study showed that not taking system interdependencies into account will underestimate operability loss and recovery time. It was also shown that that, within the constraints of this research, the strategy of recovery resource allocation had a great impact on community resilience. The impact was exacerbated when resources were insufficient. Among the six resource allocation strategies studied, the ones that adjusted based on damage/reconstruction states enhanced resilience. This points to the necessity of maximizing a community's ability to have good information flow after a disaster. In other words, the hardening of monitoring and communications systems and making them more damage-tolerant is an effective way to increase community resilience. This, of course, can only be achieved by building, prior to the event, institutional relationships that will foster cooperation between the various public and private players that would be involved in response, restoration, and recovery.

A limitation of this work lies in some of the assumptions and simplifications made. For example, the effect of delays due to bad weather conditions and traffic blockages or the effect of limited construction materials on the available number of resource units was not considered. Although these omissions and simplifications may influence the specific results presented in this paper, the framework's flexibility and extensibility permit it to address them in the future through the addition of new simulators or the modification of the existing simulators.

Data Availability Statement

All data, models, and code generated or used during the study appear in the published article.

Acknowledgments

This work was supported by the University of Michigan and the US National Science Foundation (NSF) through Grant No. ACI-1638186. Any opinions, findings, conclusions, and recommendations expressed in this paper are those of the authors and do not necessarily reflect the views of the sponsors.

References

Adachi, T., and B. R. Ellingwood. 2008. "Serviceability of earthquake-damaged water systems: Effects of electrical power availability and power backup systems on system vulnerability." *Reliab. Eng. Syst. Saf.* 93 (1): 78–88. https://doi.org/10.1016/j.ress.2006.10.014.

Adachi, T., and B. R. Ellingwood. 2009. "Serviceability assessment of a municipal water system under spatially correlated seismic intensities." *Comput. Aided Civ. Infrastruct. Eng.* 24 (4): 237–248. https://doi.org/10.1111/j.1467-8667.2008.00583.x.

Albert, R., I. Albert, and G. L. Nakarado. 2004. "Structural vulnerability of the North American power grid." *Phys. Rev. E* 69 (2): 025103. https://doi.org/10.1103/PhysRevE.69.025103.

Atkinson, G. M., and D. M. Boore. 1995. "Ground-motion relations for eastern North America." *Bull. Seismol. Soc. Am.* 85 (1): 17–30.

Barton, D. C., E. D. Eidson, D. A. Schoenwald, K. L. Stamber, and R. K. Reinert. 2000. *Aspen-EE: An agent-based model of infrastructure interdependency.* SAND2000-2925. Albuquerque, NM: Sandia National Laboratories.

Chang, S. E., and S. B. Miles. 2004. "The dynamics of recovery: A framework." In *Modeling spatial and economic impacts of disasters*, edited by Y. Okuyama and S. E. Chang, 181–204. Berlin: Springer.

Chang, S. E., H. A. Seligson, and R. T. Eguchi. 1996. *Estimation of the economic impact of multiple lifeline disruption: Memphis light, gas and water division case study.* Buffalo, NY: National Center for Earthquake Engineering Research.

Cimellaro, G. P., C. Renschler, A. M. Reinhorn, and L. Arendt. 2016. "PEOPLES: A framework for evaluating resilience." *J. Struct. Eng.* 142 (10): 4016063. https://doi.org/10.1061/(ASCE)ST.1943-541X.0001514.

Cutler, H., M. Shields, D. Tavani, and S. Zahran. 2016. "Integrating engineering outputs from natural disaster models into a dynamic spatial computable general equilibrium model of Centerville." *Sustainable Resilient Infrastruct.* 1 (3–4): 169–187. https://doi.org/10.1080/23789689.2016.1254996.

Cutter, S. L., B. J. Boruff, and W. L. Shirley. 2003. "Social vulnerability to environmental hazards." *Social Sci. Q.* 84 (2): 242–261. https://doi.org/10.1111/1540-6237.8402002.

Dudenhoeffer, D. D., M. R. Permann, and M. Manic. 2006. "CIMS: A Framework for Infrastructure Interdependency Modeling and Analysis." In *Proc., 2006 Winter Simulation Conf.*, 478–485. Piscataway, NJ: IEEE Press.

Dueñas-Osorio, L., J. I. Craig, and B. J. Goodno. 2007. "Seismic response of critical interdependent networks." *Earthquake Eng. Struct. Dyn.* 36 (2): 285–306. https://doi.org/10.1002/eqe.626.

Ellingwood, B. R., H. Cutler, P. Gardoni, W. G. Peacock, J. W. van de Lindt, and N. Wang. 2016. "The Centerville virtual community: A fully integrated decision model of interacting physical and social infrastructure systems." *Sustainable Resilient Infrastruct.* 1 (3–4): 95–107. https://doi.org/10.1080/23789689.2016.1255000.

Eusgeld, I., D. Henzi, and W. Kröger. 2008. "Comparative evaluation of modeling and simulation techniques for interdependent critical infrastructures." In *Laboratory for safety analysis*. Zurich, Switzerland: ETH Zurich.

FEMA. 2003. *Earthquake loss estimation methodology: Technical manual*. Washington, DC: National Institute of Building for the Federal Emergency Management Agency.

Ghosn, M., et al. 2016. "Performance indicators for structural systems and infrastructure networks." *J. Aerosp. Eng.* 29 (4): F4016003. https://doi.org/10.1061/(ASCE)ST.1943-541X.0001542.

González, A. D., L. Dueñas-Osorio, M. Sánchez-Silva, and A. L. Medaglia. 2016. "The interdependent network design problem for optimal infrastructure system restoration." *Comput. Aided Civ. Infrastruct. Eng.* 31 (5): 334–350. https://doi.org/10.1111/mice.12171.

Guidotti, R., H. Chmielewski, V. Unnikrishnan, P. Gardoni, T. McAllister, and J. van de Lindt. 2016. "Modeling the resilience of critical infrastructure: The role of network dependencies." *Sustainable Resilient Infrastruct.* 1 (3–4): 153–168. https://doi.org/10.1080/23789689.2016.1254999.

Hernandez-Fajardo, I., and L. Dueñas-Osorio. 2013. "Probabilistic study of cascading failures in complex interdependent lifeline systems." *Reliab. Eng. Syst. Saf.* 111 (Mar): 260–272. https://doi.org/10.1016/j.ress.2012.10.012.

Koliou, M., J. W. van de Lindt, T. P. McAllister, B. R. Ellingwood, M. Dillard, and H. Cutler. 2018. "State of the research in community resilience: Progress and challenges." *Sustainable Resilient Infrastruct.* 1–21. https://doi.org/10.1080/23789689.2017.1418547.

Lin, P., and N. Wang. 2016. "Building portfolio fragility functions to support scalable community resilience assessment." *Sustainable Resilient Infrastruct.* 1 (3–4): 108–122. https://doi.org/10.1080/23789689.2016.1254997.

Lin, S.-Y., W.-C. Chuang, L. Xu, S. El-Tawil, S. M. J. Spence, V. R. Kamat, C. C. Menassa, and J. McCormick. 2019. "A framework for modeling interdependent effects in natural disasters: Application to wind engineering." *J. Struct. Eng.* 145 (5): 04019025. https://doi.org/10.1061/(ASCE)ST.1943-541X.0002310.

Loggins, R., R. G. Little, J. Mitchell, T. Sharkey, and W. A. Wallace. 2019. "CRISIS: Modeling the restoration of interdependent civil and social infrastructure systems following an extreme event." *Nat. Hazards Rev.* 20 (3): 04019004. https://doi.org/10.1061/(ASCE)NH.1527-6996.0000326.

Miles, S. B., and S. E. Chang. 2007. *A simulation model of urban disaster recovery and resilience: Implementation for the 1994 Northridge earthquake*. Technical Rep. No. MCEER-07-0014. Buffalo, NY: Multidisciplinary Center for Earthquake Engineering Research.

Miles, S. B., and S. E. Chang. 2011. "ResilUS: A community based disaster resilience model." *Cartography Geographic Inf. Sci.* 38 (1): 36–51. https://doi.org/10.1559/1523040638136.

Moreno, J., and D. Shaw. 2019. "Community resilience to power outages after disaster: A case study of the 2010 Chile earthquake and tsunami." *Int. J. Disaster Risk Reduct.* 34 (1): 448–458. https://doi.org/10.1016/j.ijdrr.2018.12.016.

Morshedlou, N., A. D. González, and K. Barker. 2018. "Work crew routing problem for infrastructure network restoration." *Transp. Res. Part B* 118 (Dec): 66–89. https://doi.org/10.1016/j.trb.2018.10.001.

NER (National Earthquake Resilience). 2011. *National earthquake resilience: Research, implementation, and outreach*. Washington, DC: National Academies Press.

Ouyang, M. 2014. "Review on modeling and simulation of interdependent critical infrastructure systems." *Reliab. Eng. Syst. Saf.* 121 (Jan): 43–60. https://doi.org/10.1016/j.ress.2013.06.040.

PEER (Pacific Earthquake Engineering Research Center). 2018. "PEER ground motion database." Accessed January, 2018. https://ngawest2.berkeley.edu/.

Reilly, A. C., S. D. Guikema, L. Zhu, and T. Igusa. 2017. "Evolution of vulnerability of communities facing repeated hazards." *PLoS One* 12 (9): e0182719. https://doi.org/10.1371/journal.pone.0182719.

Renschler, C. S., A. E. Frazier, L. A. Arendt, G. P. Cimellaro, A. M. Reinhorn, and M. Bruneau. 2010. "Developing the 'PEOPLES' resilience framework for defining and measuring disaster resilience at the community scale." In *Proc., 9th US National and 10th Canadian Conf. on Earthquake Engineering (9USN/10CCEE)*. Oakland, CA: Earthquake Engineering Research Institute.

Rinaldi, S. M., J. P. Peerenboom, and T. K. Kelly. 2001. "Identifying, understanding, and analyzing critical infrastructure interdependencies." *IEEE Control Syst.* 21 (6): 11–25. https://doi.org/10.1109/37.969131.

Schmeltz, M. T., S. K. González, L. Fuentes, A. Kwan, A. Ortega-Williams, and L. P. Cowan. 2013. "Lessons from hurricane sandy: A community response in Brooklyn, New York." *J. Urban Health* 90 (5): 799–809. https://doi.org/10.1007/s11524-013-9832-9.

Schoenwald, D. A., D. C. Barton, and M. A. Ehlen. 2004. "An agent-based simulation laboratory for economics and infrastructure interdependency." In Vol. 1292 of *Proc., 2004 American Control Conf.*, 1295–1300. Piscataway, NJ: IEEE Press.

Shinozuka, M., X. Dong, J. Xianhe, and T. C. Cheng. 2005. "Seismic performance analysis for the LADWP power system." In *Proc.,* 2005 IEEE/PES *Transmission and Distribution Conf. and Exposition: Asia and Pacific*, 1–6. Piscataway, NJ: IEEE Press.

Song, J., and S.-Y. Ok. 2010. "Multi-scale system reliability analysis of lifeline networks under earthquake hazards." *Earthquake Eng. Struct. Dyn.* 39 (3): 259–279. https://doi.org/10.1002/eqe.938.

USGS. 2018. "Memphis, Shelby County seismic hazard maps and data." Accessed February, 2018. https://earthquake.usgs.gov/hazards/urban/memphis/grid_download.php.

Zhang, P., and S. Peeta. 2011. "A generalized modeling framework to analyze interdependencies among infrastructure systems." *Transp. Res. Part B: Methodol.* 45 (3): 553–579. https://doi.org/10.1016/j.trb.2010.10.001.

Zimmerman, R. 2001. "Social Implications of Infrastructure network Interactions." *J. Urban Technol.* 8 (3): 97–119. https://doi.org/10.1080/106307301753430764.